ARTICLE

Protein Folding Dynamics of Cytochrome *c* Seen by Transient Grating and Transient Absorption Spectroscopies

Jungkweon Choi,* Cheolhee Yang, Jeongho Kim, and Hyotcherl Ihee*

Center for Time-Resolved Diffraction, Department of Chemistry, Graduate School of Nanoscience & Technology (WCU), KAIST, Daejeon 305-701, Republic of Korea

ABSTRACT: We investigate optically triggered protein folding dynamics of cytochrome *c* (Cyt*c*) using transient grating (TG) and transient absorption (TA) spectroscopies. Despite many studies on protein folding dynamics of Cyt*c*, a well-known model protein, direct spectroscopic evidence for the three-dimensional global folding process has been rarely reported. By measuring the TG signal of CO-bound Cyt*c* (Cyt*c*−CO) in the presence of a denaturant, we clearly detected the change of diffusion coefficient that reflects the size change of Cyt*c* upon photodissociation of the CO ligand from unfolded Cyt*c*−CO. The quantitative analysis of TG signals supports that the optically triggered folding reaction of Cyt*c* in the presence of a denaturant takes place through a detectable intermediate (three-state folding kinetics). This is in contrast with the two-state folding dynamics of Cyt*c* under a denaturant-free environment without any detectable intermediate.[1] From the quantitative global analysis of the TG signals, the rate constants for the U → I and I → N transitions in a CAPS buffer solution (pH 7) at room temperature in the presence of a denaturant at various concentrations are determined to be 1065 ± 17 to 3476 ± 103 s^{-1} and 101 ± 6 to 589 ± 21 s^{-1}, respectively. In addition, the activation energies (E_a) for the U → I and I → N transitions are determined to be 8.7 ± 1.0 kcal/mol and 7.1 ± 1.3 kcal/mol, respectively. The folding dynamics of Cyt*c* initiated by the CO photolysis is discussed based in terms of the protein size change.
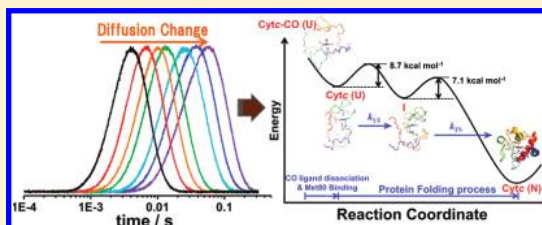
1. INTRODUCTION

Protein folding is the self-assembly of a polypeptide chain into its characteristic and functional three-dimensional (3D) structure. Proteins can perform their functions only when they have their correct 3D structures. Conversely, accumulation of misfolded proteins can cause fatal diseases such as Alzheimer's, mad cow, and Parkinson's. In this respect, an understanding of the protein folding/unfolding process is important, yet it requires detailed knowledge of protein conformational changes. To obtain such information on the protein structural changes, many experimental and theoretical efforts have been made.[2−14] In particular, time-resolved spectroscopic techniques with high sensitivity and superb time resolution have been effective in tracking protein folding processes occurring on time scales from nanoseconds to seconds. For example, time-resolved circular dichroism (CD),[3−5] IR and Raman,[6−8,15] fast mixing stopped-flow method,[16,17] transient absorption (TA) spectroscopy,[16−19] and laser-induced transient grating (TG) have been applied to studying the dynamics of protein conformational changes.[1,14,20−22] Among these spectroscopic techniques, the TG method is a unique tool that can sensitively probe the global structural changes by monitoring the change of the diffusion coefficient of a protein. This aspect of the TG technique separates itself from the other techniques that are suited for obtaining the information on the local, specific energy states or chromophores. The diffusion coefficient, D, is certainly a sensitive measure for monitoring a protein folding process because it is directly related to the size and shape of a macromolecule. Practically, in various biological

reactions such as protein folding, the diffusion coefficient reflects not only the global structural change of a biomolecule itself but also the intermolecular interaction between protein and solvent.

In this work, we investigate the optically triggered folding dynamics of CO-bound reduced cytochrome *c* (Cyt*c*−CO) in various denaturant concentrations by using laser-induced TG and TA spectroscopies. Cyt*c* is a small heme protein (∼12 kDa) and serves as an electron carrier in the electron transport chain across a membrane. Unlike other heme proteins such as myoglobin and hemoglobin, the heme iron of Cyt*c* does not bind to the CO ligand in its native state because it is bound to Met-80 residue covalently. However, in the presence of a denaturant, Met-80 can be replaced by a CO ligand, inducing the unfolding of Cyt*c*. Conversely, the folding reaction of Cyt*c* can be triggered by photoinduced dissociation of the CO ligand, as shown in Figure 1a. This optically triggered folding process of Cyt*c*−CO is a good model system for studying the protein folding process and thus has been intensively studied using TA and time-resolved CD method. However, direct spectroscopic evidence for the conformational change associated with the folding of Cyt*c* has been lacking. For example, a TA measurement of the same system mainly probed the binding of the iron-residues and the CO recombination.[18,23] In addition, the dynamics for the formation of a secondary structure and two rebinding reactions of
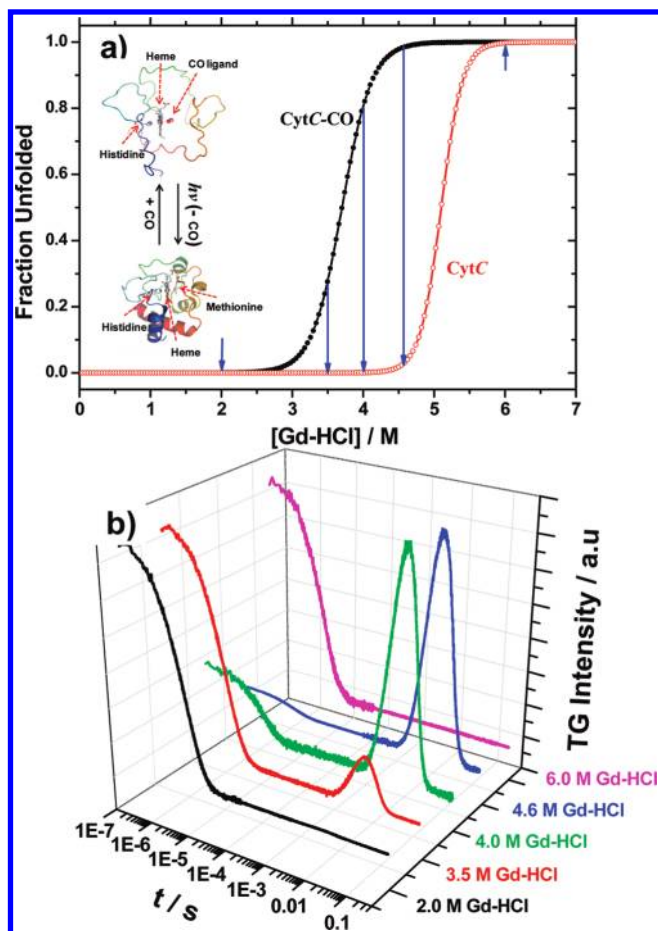
Figure 1. (a) Folding curves of Cyt$c$−CO and Cyt$c$ as a function of the concentration of Gd−HCl. The native-state structure of reduced Cyt$c$ is completely unfolded by the CO binding at an appropriate denaturant concentration. Thus, the folding dynamics of Cyt$c$ can be initiated by the photodissociation of CO ligand. These curves are taken from the data of Eaton et al. (refs 2 and 18). The arrows indicate the concentration of Gd−HCl used in our TG experiments. (b) TG signals measured by photoexcitation of 1 mM Cyt$c$−CO solution in 50 mM CAPS buffer (pH 7) containing various concentrations of Gd−HCl (from right to left, 2.0, 3.5, 4.0, 4.6, and 6.0 M Gd−HCl, and q^2 = 0.91, 0.87, 0.89, 0.86, and 0.92 × 10^{12} m$^{−2}$, respectively). The TG signals were normalized at the maximum intensity of each TG signal. The TG signals for the Cyt$c$ samples of 2.0 and 6.0 M Gd−HCl concentrations rises following the instrumental response of our system and decays on microsecond time scale, which is ascribed to the decay of thermal grating. There is no additional decay components afterward in millisecond time range as the folding cannot be initiated at these Gd−HCl concentrations. However, for the Cyt$c$ samples containing Gd−HCl in the concentration range of 3.5−4.6 M, the TG signals show strong grow−decay dynamics in millisecond time range due to the folding dynamics in addition to the thermal grating decay observed on microsecond time scale.

CO ligand were measured by a time-resolved CD experiment, but any additional slow dynamics due to the folding process of Cyt$c$ were not observed.[5]

In this paper, using the TG method, we clearly demonstrate the evidence for the size change of Cyt$c$ associated with the folding reaction. By measuring the TG signals while varying the grating wavenumber (q) and the sample temperature, we obtain the rate constant and activation energy of the Cyt$c$ folding reaction, respectively. The quantitative analysis of the measured

TG signals shows that the folding dynamics of Cyt$c$ triggered by the photodissociation of a CO ligand is well explained by a three-state folding kinetic model rather than the two-state and sequential mechanisms.

2. BACKGROUND

Principle of TG Spectroscopy. In a TG experiment, a sample is excited by spatial modulation of light intensity, i.e. transient grating, produced by the interference of two excitation light waves. The TG signal (I_{TG}) is proportional to the sum of the square of the refractive index (δn: phase grating) and/or the absorbance (δk: amplitude grating) differences between the peak and valley of the grating pattern,

$$I_{TG}(t) = \alpha[\delta n(t)]^2 + \beta[\delta k(t)]^2 \quad (1)$$

where α and β are coefficients determined by the experimental conditions. The amplitude grating (δk) arises from chemical species that absorbs the probe light. Since CO and proteins possess no absorption at the probe wavelength of 780 nm, the amplitude grating term vanishes in our case.

The δn mainly comes from (i) the thermal energy releasing process, $\delta n_{th}(t)$ and (ii) the sum of refractive index changes of each chemical species, $\sum \delta n_{spe}(t)$:

$$\delta n(t) = \delta n_{th}(t) + \sum \delta n_{spe}(t) \quad (2)$$

Therefore, the TG signal can be expressed as

$$I_{TG}(t) = \alpha[\delta n_{th}(t) + \sum \delta n_{spe}(t)]^2 \quad (3)$$

Generally, the thermal grating, $\delta n_{th}(t)$, results from the temperature change in the medium induced by the energy dissipated from the nonradiative decay of excited state population and by the enthalpy change of a reaction. If the excited state decay and the reaction are fast enough to release the thermal energy, the temporal profile of the thermal grating is given by

$$\delta n_{th}(t) = \delta n_{th} \exp(-k_{th}t) = \delta n_{th} \exp(-D_{th}q^2 t) \quad (4)$$

where D_{th} is the thermal diffusivity. A rate constant, k_{th}, which is equal to $D_{th}q^2$, allows us to readily extract the contribution of the thermal grating. On the other hand, the species grating (δn_{spe}) consists of the following two contributions; (i) the population grating (δn_{pop}) and (ii) volume grating (δn_{vol}), where δn_{pop} and δn_{vol} are the refractive changes due to the population and the volume gratings, respectively ($\delta n_{spe} = \delta n_{pop} + \delta n_{vol}$). The intensity of the species grating signal is determined by the difference in the refractive index changes due to the reactant (δn_R, unfolded Cyt$c$−CO) and the product (δn_P). Thus, the observed TG signal intensity can be expressed by

$$I_{TG}(t) = \alpha[\delta n_{th}(t) + \delta n_P(t) - \delta n_R(t)]^2 \quad (5)$$

The "product" in eq 5 stands for any chemical species produced from the reactant at the time of observation.

Application to the Folding Dynamics of Cyt$c$. The folding processes of many proteins have been often interpreted using two-state, three-state, or sequential mechanisms. In principle, a more complicated mechanism such as parallel pathways composed of a mixture of these simple mechanisms cannot be ruled out, but analysis of the TG signal considering such possibilities is

impractical due to the drastic increase of the number of fitting parameters. Nevertheless, comparison of the three simplified versions of mechanisms still should give insight into the folding mechanism. The two-state mechanism involves a transition from the unfolded to the folded state without any detectable intermediate. The folding reaction of a protein in the three-state mechanism takes place through a detectable intermediate, whereas the protein structure in the sequential mechanism continuously changes with time. We compare our data with the models for the two-state, three-state, and sequential mechanisms. First, D of Cyt$c$ in the two-state model changes abruptly between two values by the transition between unfolded and folded states. When the protein folds via the two-state mechanism with a protein folding rate, k_f, as in the following scheme,
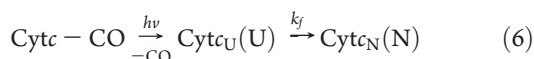
$$Cytc - CO \xrightarrow[-CO]{h\nu} Cytc_U(U) \xrightarrow{k_f} Cytc_N(N) \qquad (6)$$

the time dependence of each species is given by the following diffusion equations:

$$\frac{\partial Cytc - CO(x,t)}{\partial t} = D_{Cytc-CO}\frac{\partial^2 Cytc - CO(x,t)}{\partial x^2}$$
$$\frac{\partial U(x,t)}{\partial t} = D_U\frac{\partial^2 U(x,t)}{\partial x^2} - k_f U(x,t) \qquad (7)$$
$$\frac{\partial N(x,t)}{\partial t} = D_N\frac{\partial^2 N(x,t)}{\partial x^2} + k_f U(x,t)$$

By solving these equations assuming similar molecular sizes for Cyt$c$−CO and Cytc_U ($D_{Cytc-CO} \sim D_U$), the TG signal for the two-state model can be obtained as:

$$I_{TG}^{Two-State} =$$
$$\alpha \begin{bmatrix} -\delta n_{th} \exp(-D_{th}q^2 t) \\ -\delta n_{Cytc-CO} \exp(-D_U q^2 t) + \delta n_U \exp\{-(D_U q^2 + k_f)t\} \\ +\frac{k_f}{(D_N - D_U)q^2 - k_f}\delta n_N[\exp\{-(D_U q^2 + k_f)t\} - \exp(-D_N q^2 t)] \end{bmatrix}^2$$
$$(8)$$

where $\delta n_{Cytc-CO}$, δn_U, and δn_N are the initial refractive index changes for Cyt$c$−CO, the unfolded Cyt$c$, and the folded Cyt$c$, respectively.

Second, in the three-state mechanism, the folding reaction of a protein takes place through a detectable intermediate (I) as in the following scheme.
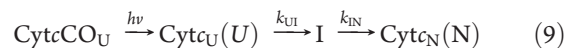
$$CytcCO_U \xrightarrow{h\nu} Cytc_U(U) \xrightarrow{k_{UI}} I \xrightarrow{k_{IN}} Cytc_N(N) \qquad (9)$$

The time-dependence of each species is given by the following diffusion equations:

$$\frac{\partial Cytc - CO(x,t)}{\partial t} = D_{Cytc-CO}\frac{\partial^2 Cytc - CO(x,t)}{\partial x^2}$$
$$\frac{\partial U(x,t)}{\partial t} = D_U\frac{\partial^2 U(x,t)}{\partial x^2} - k_{UI}U(x,t)$$
$$\frac{\partial I(x,t)}{\partial t} = D_I\frac{\partial^2 I(x,t)}{\partial x^2} + k_{UI}U(x,t) - k_{IN}I(x,t) \qquad (10)$$
$$\frac{\partial N(x,t)}{\partial t} = D_N\frac{\partial^2 N(x,t)}{\partial x^2} + k_f I(x,t)$$

By solving these equations, the TG signal for the three-state model can be expressed as follows:

$$I_{TG}^{Three-State}(t) = \alpha \begin{bmatrix} -\delta n_{th}\exp(-D_{th}q^2 t) \\ -dn_{CytcCO_U}\exp(-D_U q^2 t) + dn_{Cytc_U}\exp(-(D_U q^2 + k_{UI})t) \\ +\frac{dn_I k_{UI}}{(D_I - D_U)q^2 + k_{IN} - k_{UI}}[\exp(-D_U q^2 + k_{UI})t) - \exp(-D_I q^2 + k_{IN})t)] \\ +\frac{dn_{Cytc_N}k_{UI}k_{IN}}{(D_I - D_U)q^2 + k_{IN} - k_{UI}}\left[\frac{\exp(-D_U q^2 + k_{UI})t) - \exp(-D_N q^2 t)}{(D_N - D_U)q^2 - k_{UI}} - \frac{\exp(-D_I q^2 + k_{IN})t) - \exp(-D_N q^2 t)}{(D_N - D_I)q^2 - k_{IN}}\right] \end{bmatrix}$$
$$(11)$$

Finally, in the sequential mechanism, the protein structure continuously changes with time and therefore the D of the protein is time-dependent without any specific intermediate value. The time dependence of D can be modeled by a single exponential function with a rate constant k_f,

$$D(t) = D_U + (D_N - D_U)(1 - \exp(-k_f t)) \qquad (12)$$

where D_U and D_N are the diffusion coefficients of unfolded Cyt$c$(U) and folded Cyt$c$(N), respectively. The time-dependent $C(x,t)$ of the folded protein is governed by the following diffusion equation with time-dependent $D(t)$

$$\frac{\partial C(x,t)}{\partial t} = D(t)\frac{\partial^2 C(x,t)}{\partial x^2} \qquad (13)$$

Solving the equation provides the TG signal for the sequential model as:

$$I_{TG}^{Sequential} = \alpha \begin{bmatrix} -\delta n_{th}\exp(-D_{th}q^2 t) - \delta n_{Cytc-CO}\exp(-D_{Cytc-CO}q^2 t) \\ +\delta n_N \exp\left[-D_N q^2 t - \frac{(D_N - D_U)q^2}{k_f}(1 - \exp(-k_f t))\right] \end{bmatrix}^2$$
$$(14)$$

3. EXPERIMENTAL SECTION

Sample Preparation. Equine heart cytochrome c (Cyt$c$) was purchased from Sigma-Aldrich and dissolved in 50 mM CAPS buffer (pH 7.0) containing Gd−HCl at various concentrations. The concentrations of the Cyt$c$ solutions were adjusted to be 1 mM. The Cyt$c$ is reduced by adding 10 μL of 1 M sodium dithionite solution to the Cyt$c$ solutions under a nitrogen

atmosphere. Then, the CO gas is passed over the reduced sample for 30 min to convert the Cyt$c$ to the CO-bound Cyt$c$ (Cyt$c$—CO). For the spectroscopic measurements, the prepared solutions were put into a rubber-topped, airtight quartz cuvette of 2 mm optical path length. To ensure the freshness of the sample solutions, the spectoscopic measurements were made immediately after the sample preparation.

Diffusion Coefficient. The diffusion coefficient determined from the global fitting of TG signals after photoexcitation of Cyt$c$—CO at various Gd—HCl concentrations was corrected for the increase of the solution viscosity due to Gd—HCl as reported by Kawahara et al.[24]

Transient Grating Spectroscopy. The experimental setup for the TG experiment is similar to that reported previously.[25,26] The second harmonic (532 nm) of a Nd:YAG laser (Brilliant B, pulse width 6—7 ns) was used as an excitation beam and a photodiode beam (780 nm, Thorlabs) as a probe beam. The diffracted probe beam (TG signal) off the transient grating created by pump light was isolated from the excitation laser beam by a glass filter (Thorlabs FGL715S) and a pinhole. A photosensor module (Hamamatzu H7732—10) with a photomultiplier tube (Hamamatzu R-928) detected the isolated TG signal and a digital oscilloscope (Tektronix TDS 3052B) digitized it. The repetition rate of the photoexcitation was set to 2 Hz. The energy of the excitation beam was kept below ∼10 μJ to prevent multiphoton absorption. The TG signal was averaged 32 times to obtain a sufficient signal-to-noise ratio. The size of the excitation beam focused at the sample position was about 1 mm diameter. The laser-irradiated volume was small (typically ca. 2×10^{-3} cm^3) compared to the total volume of the sample solution. The sample cells were kept inside a temperature-controlled sample holder. All experiments were carried out at room temperature.

The value of the grating wavenumber (q) in the TG measurement is determined from the decay rate of the thermal grating signal of a reference sample, bromocresol purple (BCP), because BCP releases the energy of the absorbed photon as heat into the solvent with a quantum yield of unity. All TG measurements were carried out within a small q^2 range ($\leq 6.2 \times 10^{12}$ m^{-2}) where the folding rate of a protein is on the time scale of the same order of magnitude as the diffusion rate so that the TG signal associated with the diffusion process is more sensitive to the folding process.

Transient Absorption Spectroscopy. Transient absorption (TA) experiments were performed for 200 μM of Cyt$c$—CO solution in a CAPS buffer (pH 7) using the second harmonic (532 nm) of a Nd:YAG laser (Brilliant B, pulse width 6—7 ns) as an excitation source and a 250 W Xe lamp as a probing light source. The probing light was oriented perpendicular to the excitation laser beam, passed through a grating monochromator, and detected with a photomultiplier (Hamamatsu R-928) and a digital oscilloscope (Tektronix TDS 3052B).

4. RESULTS AND DISCUSSION

Figure 1b shows the TG signals of Cyt$c$—CO solutions in 50 mM CAPS buffer (pH 7) containing various concentrations of Gd—HCl. The TG signals from the Cyt$c$ samples of low (≤ 2 M) and high (≥ 6 M) Gd—HCl concentrations, where both Cyt$c$—CO and Cyt$c$ are completely folded or unfolded (see Figure 1a), show simple temporal decay profiles, i.e., rise rapidly following the instrumental response of our system and decay on
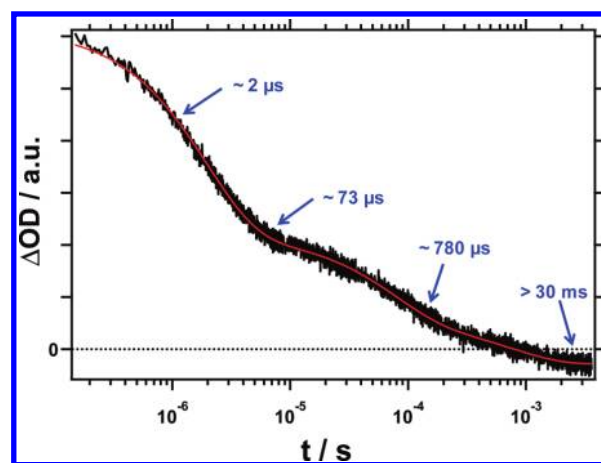

Figure 2. Transient absorption change observed at 633 nm following photolysis of 200 μM Cyt$c$—CO solution in 50 mM CAPS buffer solution (pH 7) involving 4.0 M Gd—HCl. The temporal profile of the absorbance change is expressed by a tetra-exponential function with relaxation times of ∼2 μs, ∼73 μs, ∼780 μs, and ∼30 ms. The theoretical fitting result is shown in red. According to Kliger and co-workers,[5] the first two are attributed to the binding of methionines (Met-80 or Met-65) and histidines (His-26 or His-33) to the heme iron and subsequent photodissociation of CO ligand, respectively, and the ∼780 μs process is due to the bimolecular recombination of CO and Cyt$c$. The slowest one (>30 ms) has not been reported in a previous TA studies in the literature.

microsecond time scale without any longer kinetic components. In contrast, for the samples of 3.5, 4.0, and 4.6 M Gd—HCl concentrations, where the folding of Cyt$c$ can be initiated by photodissociation of a CO ligand as shown in Figure 1a, the TG signals show additional grow—decay kinetic components in millisecond time range.

The measured TG signals can be decomposed to two contributions: thermal grating and species grating. In a TG experiment, the solute molecules excited by a periodic spatial modulation of light intensity can either (i) return to their ground state by releasing the absorbed photon energy to the solvent (heating) or (ii) undergo photoreactions that produce new chemical species, generating concentration modulations of heat and chemical species, respectively. These thermal and species gratings in turn lead to the sinusoidal modulation of the refractive index (δn), which diffracts the probe beam to give the TG signal. As a result, the TG signal intensity is proportional to the square of the sum of (i) the refractive index change due to the thermal energy releasing process ($\delta n_{th}(t)$) and (ii) the sum of refractive index changes of each chemical species ($\Sigma \delta n_{spe}(t)$), as described in eq 2. Accordingly, the TG signal intensity decreases as each of the two contributions becomes weaker. For example, the thermal grating term, $\delta n_{th}(t)$, decays by translational diffusion of heat via solvent. Since the rate constant of the $\delta n_{th}(t)$ decay is equal to $D_{th}q^2$ as shown in eq 4, it is easy to identify the thermal grating component. In the data shown in Figure 1, the decay component observed on microsecond time scale is attributed to the thermal grating. After the decay of the thermal grating signal is complete, the TG signal shows grow—decay dynamics on millisecond time scale, only for the samples containing 3.5—4.6 M Gd—HCl where the folding transition from unfolded to native state is induced by the photodissociation of the CO ligand. These results already imply that the grow—decay dynamics is related to the folding dynamics even prior to any quantitative analysis.
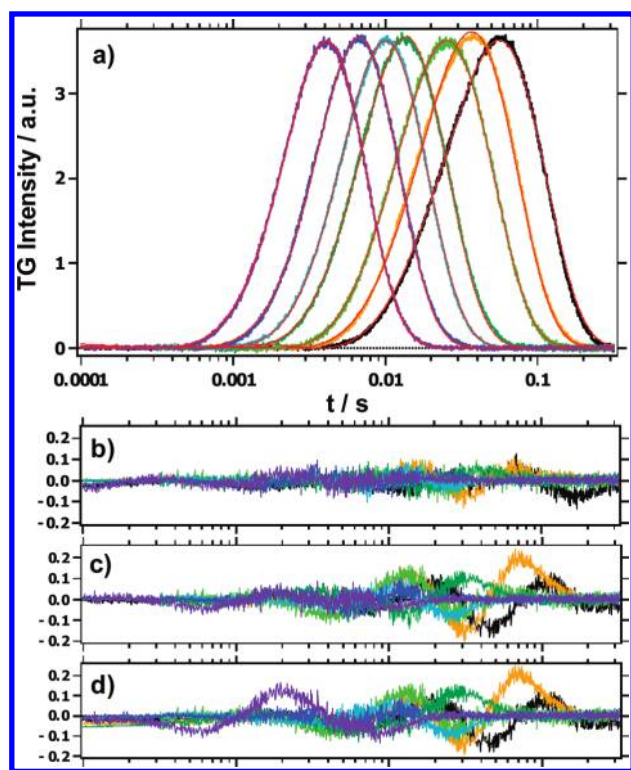
Figure 3. (a) Time profiles of the species grating signals after photo-excitation of Cyt$c$−CO in a CAPS buffer solution (pH 7) containing 4.6 M Gd−HCl at various q^2 ranges (from right to left, q^2 = 0.40, 0.63, 0.86, 1.79, 2.33, 3.74 and 6.21 × 10^{12} m^{-2}). The theoretical fits obtained from the global fitting analysis using the three-state model are shown in red. Residuals are given of the global fitting results for (b) the three-state, (c) the two-state, and (d) the sequential mechanisms, respectively. The measured TG signals are well reproduced by the three-state mechanism rather than the two-state or the sequential mechanism.

Here, it is noteworthy that TG signals measured for the samples containing various concentrations of Gd−HCl do not show any decay component arising from bimolecular recombination of CO and Cyt$c$. Since the photoreaction of Cyt$c$−CO in 2 and 6 M Gd−HCl does not involve any folding process as depicted in Figure 1a, the bimolecular recombination process of CO and Cyt$c$ should dominate. However, the measured TG signals for the solutions containing 2 and 6 M Gd−HCl show only the thermal grating component on microsecond time scale. These results indicate that TG signals contain no contribution from the bimolecular recombination of CO and Cyt$c$ under these experimental conditions and thus the TG method is not sensitive to the CO recombination process. However, this observation does not mean that the CO recombination process does not occur under our experimental conditions. For example, Kliger and co-workers used TA and time-resolved CD spectroscopies to follow the dynamics of Cyt$c$−CO with 4.6 M Gd−HCl at 40 °C and observed time-dependent absorption and CD intensity changes attributed to the processes of residue-coordination and two recombination processes of CO ligand.[5] For comparison, we also conducted a TA experiment for Cyt$c$−CO with 4.0 M Gd−HCl at room temperature, as shown in Figure 2. The temporal profile of the absorbance change in the TA signal can be well fit by a tetra-exponential function with relaxation times of ∼2 μs, ∼73 μs, ∼780 μs, and ∼30 ms. In the work by Kliger and co-workers, the first two decay components of ∼2 μs and ∼73 μs
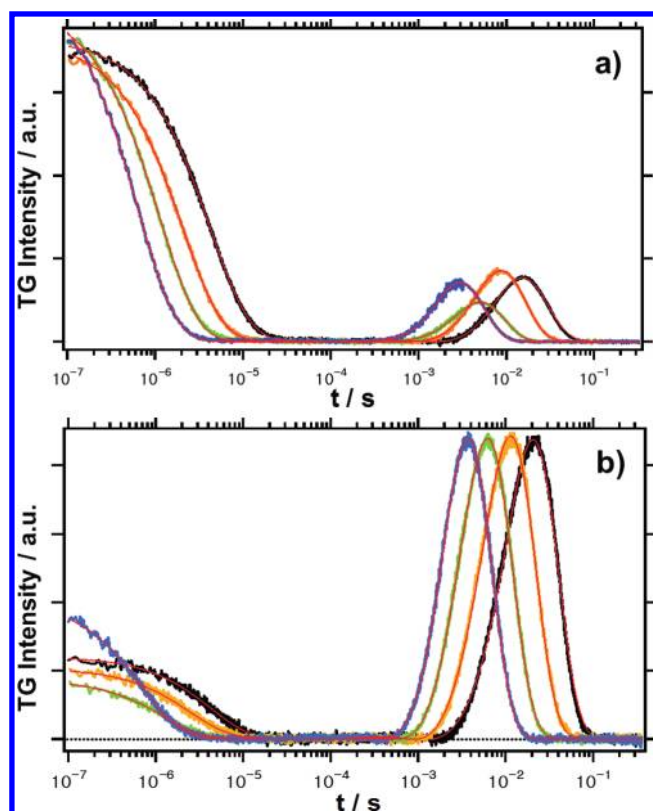

Figure 4. (a) Time profiles of the transient grating signals after photoexcitation of Cyt$c$−CO in a CAPS buffer solution (pH 7) containing 3.5 M Gd−HCl at various q^2 ranges (from right to left, q^2 = 0.87, 1.75, 3.20, and 5.61 × 10^{12} m^{-2}). (b) Time profiles of the transient grating signals after photoexcitation of Cyt$c$−CO in a CAPS buffer solution (pH 7) containing 4.0 M Gd−HCl at various q^2 ranges (from right to left, q^2 = 0.89, 1.60, 2.94, and 5.21 × 10^{12} m^{-2}). These figures show global fitting results of the whole TG signals based on the three-state model. The theoretical fits obtained from the global fitting analysis are shown in red.

time constants were assigned to the binding of methionines (Met-80 or Met-65) and histidines (His-26 or His-33) to the heme iron, respectively, upon photodissociation of the CO ligand and the ∼780 μs component was ascribed to the bimolecular recombination of CO and Cyt$c$. In contrast to others, the slowest one (∼30 ms) has never been observed in other studies. The origin of this novel component is not clear at present and will be further discussed later in this paper. These assignments imply that the TA signal is not a sensitive probe of the global structural changes such as protein folding. Overall, the TG and TA spectroscopies give the information complementary to each other, and at this point, one can conclude that the grow−decay dynamics observed in TG signals is related to the folding process of Cyt$c$.

In order to further examine the folding dynamics of Cyt$c$ induced by the photodissociation of the CO ligand, we measured the TG signals at various q^2 values for the Cyt$c$−CO sample containing 4.6 M Gd−HCl, as shown in Figure 3. With decreasing q^2 values, the grow−decay dynamics on millisecond time scale become slower, indicating that this dynamics are attributed to the diffusion processes of chemical species because the rate constant of the TG signal is given by D_iq^2 ($k_i = D_iq^2$), where D_i is the diffusion coefficient of i species. Considering that the processes of CO-ligand releasing and folding of Cyt$c$ are involved

3131

dx.doi.org/10.1021/jp106588d |*J. Phys. Chem. B* 2011, 115, 3127–3135

Table 1. D_U, D_I, D_N, k_{UI} and k_{IN} Values Determined from the Global Fitting of the TG Signals Obtained by Photoexcitation of Cytc−CO at Various Gd−HCl Concentrations and Comparison with the Values Obtained from Previous Studies in the Literature

	Cytc in pH 7 with 3.5 M Gd−HCl triggered by CO photolysis	Cytc in pH 7 with 4.0 M Gd−HCl triggered by CO photolysis	Cytc in pH 7 with 4.6 M Gd−HCl triggered by CO photolysis	Cytc in pH 13 without Gd−HCl triggered by CO photolysis[a]	Cytc in pH 7 with Gd−HCl triggered by electron transfer[b]
$D_U/m^2\,s^{-1}$	0.51×10^{-10} $(0.62 \times 10^{-10})^e$	0.42×10^{-10} $(0.54 \times 10^{-10})^e$	0.34×10^{-10} $(0.47 \times 10^{-10})^e$	0.79×10^{-10}	$0.66 \times 10^{-10c,e}$
$D_I/m^2\,s^{-1}$	0.70×10^{-10} $(0.85 \times 10^{-10})^e$	0.57×10^{-10} $(0.73 \times 10^{-10})^e$	0.37×10^{-10} $(0.50 \times 10^{-10})^e$	-	-
$D_N/m^2\,s^{-1}$	0.92×10^{-10} $(1.12 \times 10^{-10})^e$	0.73×10^{-10} $(0.93 \times 10^{-10})^e$	0.51×10^{-10} $(0.69 \times 10^{-10})^e$	1.30×10^{-10}	$1.2 \times 10^{-10d,e}$
k_{UI}/s^{-1}	2893 ± 109	3476 ± 103	1065 ± 17	256 ± 5	22
k_{IN}/s^{-1}	101 ± 6	589 ± 21	127 ± 2		

[a] These values are taken from ref 1. [b] These values are taken from the ref 14. [c] This value was determined for unfolded Cytc (Fe^{3+}) in 3.5 M Gd−HCl solutions. [d] This value was determined for folded Cytc (Fe^{2+}) in 1 M Gd−HCl solutions. [e] The D values corrected for the increase of the solution viscosity by adding Gd−HCl (corresponding to D at 0 M Gd−HCl).

in the photoinduced reaction of Cytc−CO, the following four chemical species can contribute to the species grating signal: unfolded Cytc−CO, unfolded Cytc, folded Cytc, and CO. Since the molecular sizes of unfolded Cytc−CO and unfolded Cytc are very similar, the diffusion coefficients of the two species are similar. Furthermore, since any species grating contribution from CO was not exhibited in the TG signal as explained above, the grow−decay profiles in the millisecond time range is likely to be related to the diffusion processes of unfolded Cytc and folded Cytc. From the qualitative analysis of the grow−decay profiles in millisecond time range, we confirmed that the values of the diffusion coefficients obtained from the rise and decay components are significantly different, implying the grow−decay profiles in millisecond time range is attributed to the diffusion processes of unfolded Cytc and the photoproduct such as the folded Cytc produced by the folding reaction of Cytc following after the photodissociation of CO ligand. Therefore, we analyzed the TG signal based on the folding mechanism. That is, the TG signal due to the folding reaction of Cytc can be analyzed with the definite folding kinetics in terms of the change of the diffusion coefficient of a protein.

As mentioned previously, folding processes of most proteins can be interpreted by two-state, three-state or sequential mechanisms. We compare our data with all three models. Using equations expressed from the three folding mechanisms (eq 8, 11, and 14), we fit all the TG signals by minimizing the discrepancy between the experiment and theory for all q^2 values used in the measurements. The results of this global fitting analysis are depicted in Figure 3. The measured TG signals are better fit by the three-state mechanism than the two-state or the sequential mechanism, supporting that the folding reaction of Cytc takes place following three-state folding kinetics. Furthermore, the time profiles of the TG signals for the samples containing 3.5 and 4.0 M Gd−HCl are also better fit by three-state mechanism than by the two-state and the sequential mechanism (see Figure 4). The determined parameters are summarized in Table 1. This analysis result indicates that the folding process of Cytc induced by the photodissociation of CO ligand in the presence of a denaturant takes place through a three-state mechanism. In contrast, it was reported that the folding dynamics of Cytc under a denaturant-free environment occur via a two-state mechanism.[1] Our three-state mechanism agrees with the results of previous works by Segel et al.[27] and Roder et al.[28] In the small-angle X-ray scattering study on Cytc with varying concentrations of Gd−HCl at neutral pH, Segel et al. showed that at least three equilibrium states exist for the protein: one
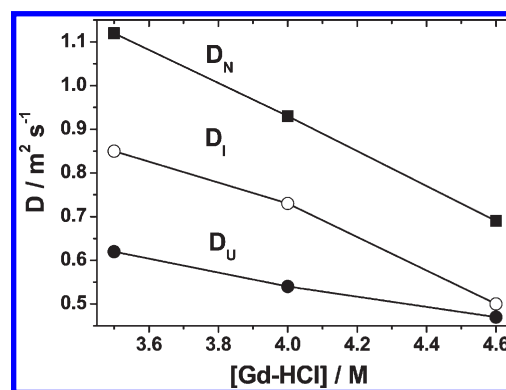
Figure 5. Changes of the diffusion coefficient, D, of the unfolded Cytc, intermediate (I) and folded Cytc as a function of the concentration of Gd−HCl.

native state (N) and two unfolded states with U_2 being fully unfolded and U_1 having some residual folding structure. In another work, Roder et al. suggested the existence of an intermediate (M), which has a compact structure distinct from that of the native state, in the folding reaction of Cytc. We note that, although the three-state mechanism gives the best agreement among the tested mechanisms, the agreement is not perfect. This leaves the possibility that the actual mechanism may not be a simple one-way, three-state pathway but a more complex mechanism including parallel pathways.

The diffusion coefficients of unfolded and folded Cytc, D_U and D_N, that were determined from the global fitting show linear dependence on the concentration of Gd−HCl, as depicted in Figure 5. As reflected in Figure 1, in the range of 3.5 − 4.6 M Gd−HCl concentration, the secondary structure of Cytc is completely formed regardless of the Gd−HCl concentration, but D_N as well as D_U still sensitively varies with the concentration of Gd−HCl. This finding suggests that the tertiary structure of Cytc considerably varies depending on the denaturant concentration whereas the secondary structure of Cytc does not. The D_N ($1.12 \times 10^{-10}\,m^2\,s^{-1}$) at 3.5 M Gd−HCl determined from the global fitting agrees with that of the native Cytc reported previously (1.2−$1.3 \times 10^{-10}\,m^2\,s^{-1}$),[14,15,29] indicating that the folded Cytc formed by the CO ligand photodissociation at 3.5 M Gd−HCl has a native-like structure. The D_U ($0.61 \times 10^{-10}\,m^2\,s^{-1}$) at 3.5 M Gd−HCl is similar to, but D_U ($0.47 \times 10^{-10}\,m^2\,s^{-1}$) at 4.6 M is significantly smaller than that of unfolded oxidized Cytc (Fe^{3+}) ($0.66 \times 10^{-10}\,m^2\,s^{-1}$) determined using a combination of

the electron transfer of NADH and TG by Terazima and co-workers.[30] This difference in diffusion coefficients indicates that the structure of unfolded reduced Cyt*c* (Fe^{2+}) at 4.6 M Gd—HCl can be different from that of unfolded oxidized Cyt*c* (Fe^{3+}). This difference is supported by a circular dichroism study by Kliger and co-workers that demonstrated that even the secondary structure of unfolded oxidized Cyt*c* (Fe^{3+}) significantly differs from that of unfolded reduced Cyt*c* —CO (Fe^{2+}).[5] On the other hand, D_U (0.79×10^{-10} m^2 s^{-1}) at pH 13 without a denaturant reported from a previous study[1] is considerably larger than D_U (0.47—0.62×10^{-10} m^2 s^{-1}) at pH 7 with a denaturant determined in this study, indicating that the unfolded Cyt*c* at pH 13 without a denaturant is relatively more folded than that at pH 7 with a denaturant.

Here, it is notable that D_N (0.69×10^{-10} m^2 s^{-1}) determined at 4.6 M Gd—HCl is much smaller than that in 3.5 M Gd—HCl, indicating that the CO photodissociation at 4.6 M Gd—HCl does not induce full folding of Cyt*c*. Although Jones et al. reported that the photodissociation reaction of the CO ligand in 4.6 M Gd—HCl solutions can induce full folding reaction of Cyt*c*,[18] Kliger et al.[5] and Arcovito et al.[23] suggested that the folding reaction under the same experimental condition is prohibited by a competition with the CO rebinding reaction or the base elimination process. Our results clearly resolve this issue by showing that the folding reaction at 4.6 M Gd—HCl leads to the formation of partially folded structure while Cyt*c* is fully folded at 3.5 M Gd—HCl via the three-state mechanism. On the other hand, the diffusion coefficients of an intermediate (I), D_I's, determined from the global fitting at 3.5 and 4.0 M Gd—HCl concentrations are larger than the D_U determined at each of the Gd—HCl concentration, indicating that the intermediate has a more folded structure compared with that of the unfolded Cyt*c*.

We now discuss the rate constant for the Cyt*c* folding process initiated by the CO photodissociation. From the quantitative global analysis of the TG signals, the rate constants of the transition from the intermediate to the folded Cyt*c* in CAPS buffer (pH 7) containing a denaturant is determined to be 101 ± 6 to 589 ± 21 s^{-1} (equal to the time constants of 9.9—1.7 ms), whereas the transition from the unfolded state to the intermediate takes place with the rate constants of 1065 ± 17 to 3476 ± 103 s^{-1} ($0.9 - 0.3$ ms time constants). These results indicate that the conformational change of Cyt*c* in terms of the size (or shape) is complete within the time scale of a few milliseconds. The rate constant for the I $\rightarrow$ N transition at 4.6 M Gd—HCl (127 s^{-1}) is greatly smaller than that reported by Jones and co-workers (1000 s^{-1}) using the TA experiment and SVD analysis.[18] Recently, Bhuyan et al. reported that the folding processes of ferrocytochrome *c* and Cyt*c*—CO monitored by fluorescence take place through the two-state mechanism with the rate constants of 501 and 912 s^{-1}, respectively.[31] These folding rate constants are larger than that determined in this study. This discrepancy is probably due to the difference in experimental conditions and probing methods because the folding kinetics of a protein tends to be very sensitive to the refolding condition and the probing technique.

Here, it is noteworthy that the dynamics of ~30 ms time constant observed in our TA experiment is much slower than the rate constant for the I $\rightarrow$ N transition measured from the TG experiment. This observation suggests that there might be an additional process after the folding of Cyt*c*, which occurs on the time scale of a few milliseconds.[32] On the other hand, the rates for the U $\rightarrow$ I and I $\rightarrow$ N folding transitions are determined to be
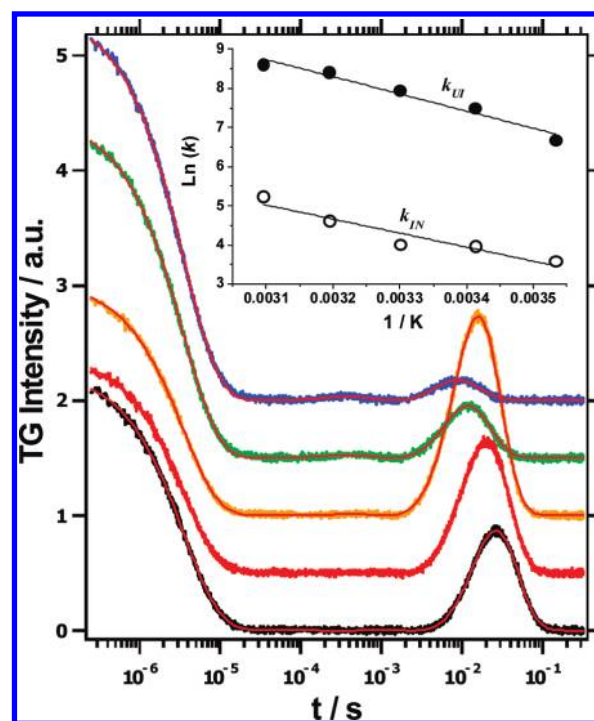

Figure 6. TG signals after photoexcitation of Cyt*c*—CO in 4.6 M Gd—HCl at $q^2 = 1.0 \times 10^{12}$ m^{-2} as a function of temperature (from top to bottom, T = 323, 313, 303, 293, and 283 K). The inset shows the temperature dependence of the folding rate constants determined from the fitting of TG signals. The activation energy (E_a) for the U $\rightarrow$ I and I $\rightarrow$ N transitions are determined to be 8.7 and 7.1 kcal/mol, respectively.

significantly slower than those of the binding of His-26, His-33, and Met-80 (or Met-65) residues to the heme iron upon the photodissociation of CO ligand. These results imply that the initial collapse associated with the binding of the His and Met residues to the heme iron does not result in the detectable change of diffusion coefficient of a protein.

To determine the activation energy (E_a) for the folding reaction of Cyt*c*, we carried out the TG experiments for the sample containing 4.6 M Gd—HCl at various temperatures, as shown in Figure 6. Using the Arrhenius equation, $E_a = -RT \ln(k_f/A)$, the activation energies (E_a) for the U $\rightarrow$ I and I $\rightarrow$ N transitions are determined to be 8.7 ± 1.0 kcal/mol and 7.1 ± 1.3 kcal/mol, respectively. In addition, the pre-exponential factors (A) for the U $\rightarrow$ I and I $\rightarrow$ N transitions are determined to be $5.1 \pm 0.4 \times 10^9$ s^{-1} and $1.0 \pm 0.1 \times 10^7$ s^{-1}, respectively. For comparison, in a previous study, we reported that the folding dynamics from the partially folded Cyt*c* to the native state Cyt*c* under a denaturant-free environment occurs via the two-state folding mechanism.[1] In the same study, the folding rate constant of Cyt*c* in the absence of a denaturant was determined to be 256 ± 5 s^{-1}, and E_a and A for the folding reaction of Cyt*c* were calculated to be 21.8 ± 1.5 kcal/mol and $7.6 \pm 0.7 \times 10^{18}$ s^{-1}, respectively.[1] The folding energy barrier of 15.8 kcal/mol ($E_{a, total} = E_{a, U \rightarrow I} + E_{a, I \rightarrow N}$) determined at 4.6 M Gd—HCl concentration is smaller than that in the absence of a denaturant (21.8 kcal/mol), supporting that the folding reaction of Cyt*c* takes place more easily in the presence of a denaturant than in the absence of a denaturant. On the other hand, the TG intensity of the grow—decay dynamics arising from the folding process of Cyt*c* significantly decreases upon increasing the temperature, as
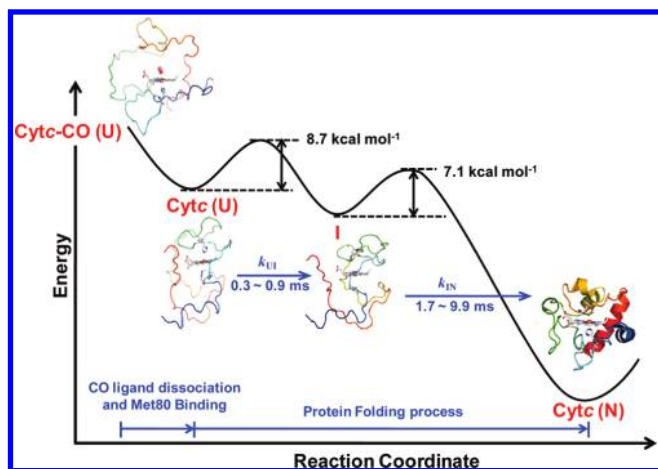
Figure 7. Schematic illustration of the folding reaction of Cyt*c* initiated by the photodissociation of CO ligand in the presence of a denaturant. The initial collapse including the binding of Met-80 to the heme iron followed by the photodissociation of CO ligand takes place without any change of diffusion coefficient of the protein on microsecond time scale, and the following folding dynamics of Cyt*c* proceeds with three-state folding kinetics on millisecond time scale.

shown in Figure 6. This temperature dependence indicates that the folding process of Cyt*c* initiated by the photodissociation of CO occur less efficiently at higher temperatures. Indeed, from a comparative time-resolved CD experiment on Cyt*c*−CO at room temperature and 40 °C, the CD signal at 220 nm, which corresponds to the native reduced CytC, is significantly enhanced at room temperature compared to at 40 °C.[5] This result supports that the folding process of Cyt*c* initiated by the photodissociation of CO takes place efficiently at room temperature. In this study, all the experiments were carried out at room temperature in 50 mM CAPS buffer solution (pH 7) to stabilize the native state (or folding intermediates), while other studies were performed at 40 °C in 100 mM phosphate buffer solution. Consequently, we were able to detect the folding process of Cyt*c* more easily.

5. CONCLUSIONS

We have studied the optically triggered folding dynamics of Cyt*c*−CO with the transient grating technique and transient absorption spectroscopy. After the photodissociation of the CO ligand from unfolded Cyt*c*−CO in the presence of a denaturant Gd−HCl, the TG signal clearly shows a change in the diffusion coefficient, D, of Cyt*c* due to the protein folding reaction. A quantitative analysis of the TG signal detected as the change of the diffusion coefficient supports that the folding process of Cyt*c* initiated by the photodissociation of CO takes place via a three-state folding mechanism with a detectable intermediate rather than a two-state or a sequential mechanism. The initial collapse including the binding of Met-80 to the heme iron following the photodissociation of CO ligand takes place without any change of the diffusion coefficient of the protein on microsecond time scale, and the following folding dynamics of Cyt*c* proceeds with three-state folding kinetics on millisecond time scale, as summarized in Figure 7. Furthermore, D of the unfolded and folded Cyt*c* decrease with increasing denaturant concentration whereas the circular dichroism intensity stays constant in the range of 3.5 − 4.6 M Gd−HCl concentration. This observation suggests that

the tertiary structure of Cyt*c* has considerable variations depending on the denaturant concentration whereas the secondary structure of Cyt*c* does not. From the quantitative global analysis of the TG signals, the rate constant of the transition from the intermediate to the folded state in a CAPS buffer solution (pH 7) involving denaturant is determined to be 101 ± 6 to 589 ± 21 s^{-1}, whereas the transition from the unfolded state to the intermediate takes place with a rate constant of 1065 ± 17 to 3476 ± 103 s^{-1}. Furthermore, the activation energy (E_a) for the U → I and I → N transitions are determined to be 8.7 ± 1.0 kcal/mol and 7.1 ± 1.3 kcal/mol, respectively.

■ AUTHOR INFORMATION

Corresponding Author
*E-mail: (J.C.) cjkbabo@gmail.com; (H.I.) hyotcherl.ihee@kaist.ac.kr.

■ REFERENCES

(1) Choi, J.; Jung, Y. O.; Lee, J. H.; Yang, C.; Kim, B.; Ihee, H. *ChemPhysChem* **2008**, *9*, 2708.
(2) Eaton, W. A.; Thompson, P. A.; Chan, C. K.; Hage, S. J.; Hofrichter, J. *Structure* **1996**, *4*, 1133.
(3) Chen, E.; Goldbeck, R. A.; Kliger, D. S. *J. Am. Chem. Soc.* **2004**, *126*, 11175.
(4) Chen, E.; Wittung-Stafshede, P.; Kliger, D. S. *J. Am. Chem. Soc.* **1999**, *121*, 3811.
(5) Chen, E.; Wood, M. J.; Fink, A. L.; Kliger, D. S. *Biochemistry* **1998**, *37*, 5589.
(6) Gilmanshin, R.; Williams, S.; Callender, R. H.; Woodruff, W. H.; Dyer, R. B. *Proc. Natl. Acad. Sci. U.S.A.* **1997**, *94*, 3709.
(7) Heitbrink, D.; Sigurdson, H.; Bolwien, C.; Brzezinski, P.; Heberle, J. *Biophys. J.* **2002**, *82*, 1.
(8) Kim, J.; Park, J.; Lee, T.; Lim, M. *J. Phys. Chem. B* **2009**, *113*, 260.
(9) Goldbeck, R. A.; Thomas, Y. G.; Chen, E.; Esquerra, R. M.; Kliger, D. S. *Proc. Natl. Acad. Sci. U.S.A.* **1999**, *96*, 2782.
(10) Hoang, L.; Bedard, S.; Krishna, M. M.; Lin, Y.; Englander, S. W. *Proc. Natl. Acad. Sci. U.S.A.* **2002**, *99*, 12173.
(11) Mines, G. A.; Pascher, T.; Lee, S. C.; Winkler, J. R.; Gray, H. B. *Chem. Biol.* **1996**, *3*, 491.
(12) Rhee, Y. M.; Sorin, E. J.; Jayachandran, G.; Lindahl, E.; Pande, V. S. *Proc. Natl. Acad. Sci. U.S.A.* **2004**, *101*, 6456.
(13) Winkler, J. R. *Curr. Opin. Chem. Biol.* **2004**, *8*, 169.
(14) Nishida, S.; Nada, T.; Terazima, M. *Biophys. J.* **2005**, *89*, 2004.
(15) Sivakolundu, S. G.; Mabrouk, P. A. *J. Am. Chem. Soc.* **2000**, *122*, 1513.
(16) Bhuyan, A. K.; Kumar, R. *Biochemistry* **2002**, *41*, 12821.
(17) Bhuyan, A. K.; Rao, D. K.; Prabhu, N. P. *Biochemistry* **2005**, *44*, 3034.
(18) Jones, C. M.; Henry, E. R.; Hu, Y.; Chan, C. K.; Luck, S. D.; Bhuyan, A.; Roder, H.; Hofrichter, J.; Eaton, W. A. *Proc. Natl. Acad. Sci. U.S.A.* **1993**, *90*, 11860.
(19) Silkstone, G.; Jasaitis, A.; Vos, M. H.; Wilson, M. T. *Dalton Trans* **2005**, 3489.
(20) Hirota, S.; Fujimoto, Y.; Choi, J.; Baden, N.; Katagiri, N.; Akiyama, M.; Hulsker, R.; Ubbink, M.; Okajima, T.; Takabe, T.; Funasaki, N.; Watanabe, Y.; Terazima, M. *J. Am. Chem. Soc.* **2006**, *128*, 7551.

(21) Nakasone, Y.; Ono, T.-a.; Ishii, A.; Masuda, S.; Terazima, M. *J. Am. Chem. Soc.* **2007**, *129*, 7028.

(22) Terazima, M. *Phys. Chem. Chem. Phys.* **2006**, *8*, 545.

(23) Arcovito, A.; Gianni, S.; Brunori, M.; Travaglini-Allocatelli, C.; Bellelli, A. *J. Biol. Chem.* **2001**, *276*, 41073.

(24) Kawahara, K.; Tanford, C. *J. Biol. Chem.* **1966**, *241*, 3228.

(25) Baden, N.; Terazima, M. *J. Phys. Chem. B* **2006**, *110*, 15548.

(26) Nada, T.; Terazima, M. *Biophys. J.* **2003**, *85*, 1876.

(27) Segel, D. J.; Fink, A. L.; Hodgson, K. O.; Doniach, S. *Biochemistry* **1998**, *37*, 12443.

(28) Latypov, R. F.; Maki, K.; Cheng, H.; Luck, S. D.; Roder, H. *J. Mol. Biol.* **2008**, *383*, 437.

(29) Fuh, C. B.; Levin, S.; Giddings, J. C. *Anal. Biochem.* **1993**, *208*, 80.

(30) Nishida, S.; Nada, T.; Terazima, M. *Biophys. J.* **2004**, *87*, 2663.

(31) Prabhu, N. P.; Kumar, R.; Bhuyan, A. K. *J. Mol. Biol.* **2004**, *337*, 195.

(32) Cammarata, M.; Levantino, M.; Schotte, F.; Anfinrud, P. A.; Ewald, F.; Choi, J.; Cupane, A.; Wulff, M.; Ihee, H. *Nat. Methods* **2008**, *5*, 881.

3135

dx.doi.org/10.1021/jp106588d |*J. Phys. Chem. B* 2011, 115, 3127–3135